Reexamination of Convective Diffusion/Drug Dissolution in a Laminar Flow Channel: Accurate Prediction of Dissolution Rate

Paul J. Missel,[1,3] Larry E. Stevens,[1] and John W. Mauger[2]

Received December 23, 2004; accepted May 3, 2004

Purpose. The convective diffusion/dissolution theory applied to flow-through dissolution in a laminar channel was reexamined to evaluate how closely it can predict release rate for a model compound on an absolute basis—a comparsion that was lacking from the original literature observations reported from this technique.

Methods. The theory was extended to allow for a finite flux of dissolving material, replacing the fixed concentration by a flux condition on the dissolving surface. The derivation introduces a new parameter, k_s, an area-independent analog of the dissolution rate constant defined in the USP intrinsic dissolution procedure.

Results. The release rate for ethyl-*p*-aminobenzoate originally observed fell within 10% of the absolute prediction assuming a solubility limited situation, and deviated from this prediction in a manner possibly consistent with a finite flux-limited condition, with $k_s \approx 10^{-4}$ M s^{-1}. For materials exhibiting lower k_s values, the derivation suggests that at high flow rates, a limit occurs where dissolution rate becomes independent of shear rate and merely a function of solubility and surface area.

Conclusions. The new parameter k_s may be deduced from any set of geometric and flow conditions, provided the fluid velocity can be determined everywhere in the domain.

KEY WORDS: convective diffusion; dissolution; dissolution rate; intrinsic dissolution rate; flow-through dissolution.

[1] Drug Delivery, Alcon Research Ltd., Fort Worth, Texas 76134, USA.
[2] University of Utah, Salt Lake City, Utah 84112, USA.
[3] To whom correspondence should be addressed. (e-mail: paul.missel@alconlabs.com)

ABBREVIATIONS: A, area of exposed dissolving surface; b, width of exposed drug surface; perpendicular to flow; BC_1, boundary condition along dissolving surface; BC_2, boundary condition at the spatial limit of the domain furthest away from the dissolving surface in the z direction; BC_3, boundary condition at the vertical boundary for the fluid inlet; C, concentration of solute; C_0, solubility of solute; D, diffusivity of solute; E, intermediate factor used in expansion expressions for R_{total}; H, height of rectangular channel; k, area averaged intrinsic solubility constant from the rotating disk method; k_s, area independent constant proposed from applying a flux boundary condition on the dissolving surface; L, length of exposed drug surface, parallel to flow; dM/dt, rate of mass lost per unit time; Q, volumetric flow rate in channel; Q_{90}, volumetric flow rate required to bring the dissolution rate up to 90% of the infinite flow rate limit; R, rate of dissolution at a particular point on the exposed drug surface; R_{total}, total integrated rate of dissolution across entire exposed drug surface; t, time; $\bar{V}$, vector describing liquid flow; W, width of rectangular channel; x, cartesian coordinate along direction of flow, parallel to dissolving surface; y, Cartesian coordinate perpendicular to direction of flow, parallel to dissolving surface; z, Cartesian coordinate perpendicular to direction of flow, perpendicular to dissolving surface; α, shear rate in boundary layer; γ_1,γ_2, functions of x which are used in deriving an approximate expression for C(x,z); $\Gamma(\ )$, gamma function; η, dimensionless spatial variable; ϕ, transformation of solute concentration as a function of spatial variable η; ξ, estimate of the distance along the releasing surface from the origin at which the dissolution upstream equals the dissolution downstream from this point.

INTRODUCTION

The currently accepted USP techniques for dissolution (1,2) and drug release (3) can be problematic when attempting to apply them to measuring the dissolution of sparingly soluble compounds or to characterize the release properties of a sustained release implant. Analytical difficulties arise from the low solute concentrations for sparingly soluble compounds such as Anecortave acetate (4,9(11)-pregnadien-17,21-diol-3,20-dione-21-acetate, CAS Registry no. 7753-60-8,MW 386), an angiostatic cortisene and investigational new drug (4) (24-month clinical outcome and safety data presented at the American Acadmeny of Ophthalmology Meeting, November 2003, presentations PA060 and PO282).

Further, the geometry and hydrodynamic conditions are suboptimal for such dosage forms. During the formative stages of development for compendial dissolution testing methods beginning in the 1960s, incomplete understanding of dissolution mechanisms led to development of a particular set of test procedures. Fluid flow patterns established in the earliest test apparatus were not studied in detail before being incorporated into a compendial protocol. It was hoped that the reliable reproduction of these poorly understood flow patterns by careful definition and standardization of test jig geometry would be sufficient for nearly all cases. This "one test fits all" approach might work well for a limited range of more highly soluble compounds or more rapidly releasing devices, but does not serve our current purpose well.

Dissolution rates are the result of a combination of intrinsic and extrinsic factors of the experiments conducted to measure these rates. Intrinsic factors pertain to properties of the drug solid state, such as crystallinity, amorphism, polymorphism, hydration, solvation, and so forth. Extrinsic factors pertain to properties of the experimental test conditions, such as temperature, fluid viscosity, pH of the medium, fluid flow, and resulting shear over the exposed surface area of the dissolving drug. There is a natural association of nomenclature between the concept of intrinsic dissolution and a particular experimental technique for measuring dissolution rate, namely, the USP rotating disk (2) method described long ago by Wood *et al.* (5).

The rotating disk method is advantageous because it controls the exposed surface area at a fixed value throughout the measurement process, and a fortuitous combination of geometry and rheology enables the entire surface to be uniformly accessible to the dissolution medium. Thus, apart from the negligible influence of edge effects, the rate of mass loss per unit surface area can be considered tantamount to a measurement of a fundamental physicochemical rate of dissolution—hence the term, intrinsic dissolution rate. However, the method suffers from limitations that preclude its application for our purpose:

1) It requires the repeated measurement of drug concentration in aliquots removed from the stirred bulk solution, and a calculation of the rate of dissolution from the slope, allowing for the introduction of errors from measurement uncertainty and chemical change of dissolved drug in the bulk environment with time.

2) Attributing the observed rate to intrinsic dissolution assumes that the solute concentration at the dissolving surface

0724-8741/04/1200-2300/0

can be maintained at the solubility limit irrespective of applied hydrodynamic conditions (6).

The current analysis overcomes these difficulties. A flow-through method allows for an instantaneous measurement of dissolution rate and an instantaneous assessment of equilibration under an applied flow, especially when the dissolution medium outlet can be directly interfaced with automated analytical equipment, and enables measurement to proceed before subsequent chemical changes can occur in solution. When it is assumed that the surface concentration is held constant at the solubility limit, the mathematical analysis is exact. The test geometry applies a uniform shear rate across the dissolving surface whose area is held constant throughout the experiment. Although the area is not uniformly accessible to the dissolution process in the same manner as for the rotating disk, a rigorous mathematical solution can be obtained (7,8) for this problem in laminar flow. This solution has been extended by relaxing the constraint of a fixed surface concentration.

Almost 30 years ago, Nelson and Shah (7,8) proposed an experimental paradigm that provides determinations of dissolution rates in a manner that does not confound the processes of molecular diffusion and forced convection. This approach has not been adopted in any compendial test. Reexamination of this method and a new comparison of the experimental data comparing release with the theoretical prediction in absolute terms has led to a more fundamental understanding of the flow-through dissolution process, by proposing a new physical constant related to the concept of intrinsic dissolution rate.

MATERIALS AND METHODS

The flow-through dissolution cell used by Shah and Nelson (7) (Fig. 1) provides for very simple geometry and set of hydrodynamic conditions. Steady (presumed) laminar flow of eluent occurs through a rectangular channel. Dissolving material (the drug used in Ref.e 7 was ethyl-*p*-aminobenzoate) is embedded flush with the channel wall by means of a dye bolted to the floor. The opening in the dye, to which a flat surface of drug is exposed to fluid flow, is rectangular, with a length to width ratio of 8:1. This geometry enabled the exact calculation to the convective diffusion-dissolution equation Eq. 1 given by Levich (9), because the fluid velocity can be solved exactly everywhere within the rectangular chamber.

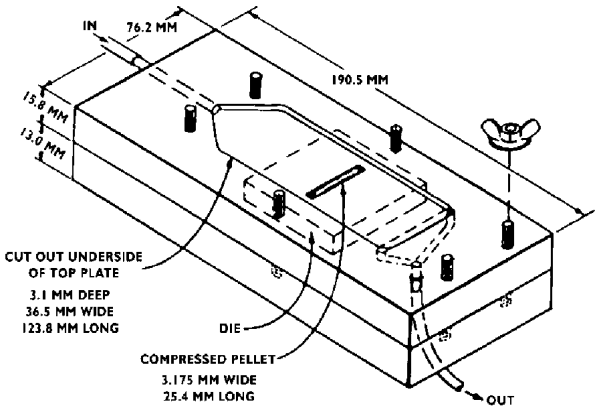

Fig. 1. Schematic diagram of dissolution cell used in Ref. 7.

(Here D is diffusion coefficient, C is scalar concentration, $\vec{V}$ is vector fluid velocity.) Apart from the rather insignificant edge effects caused by dispersion of diffusing compound, the exact solution for the dissolution rate R_{total} (rate for total mass loss from the entire exposed dissolving surface) is given (7) by Eq. 2, where C_0 is the drug solubility limit, b and L are the width and length, respectively, of the rectangular dye opening, and α is the shear rate given by Eq. 3, with Q as the volumetric flow rate and H and W are the width and height of the channel.

$$\nabla \cdot (D\nabla C) = \bar{v} \cdot \nabla C \tag{1}$$

$$R_{total} = 0.808 D^{2/3} C_0 \alpha^{1/3} b L^{2/3} \tag{2}$$

$$\alpha = \frac{6Q}{H^2 W} \tag{3}$$

The dye can be oriented in either direction and provides an important test of the theory in that, according to Eq. 2, the dissolution rate should be twice as fast when the long axis is perpendicular to the direction of flow compared to when it is parallel to the flow for an aspect ratio of 8:1.

The exact result of Eq. 2 requires that the exposed drug surface concentration be maintained at the solubility limit irrespective of flow rate, that is the boundary condition on the dissolving surface in the plane perpendicular to the floor along the direction of flow is simply $C(x,z)|_{z=0} = C_0$. This condition is rather idealistic, and it seems plausible that this condition could not be maintained regardless of flow conditions. As flow rate increases, one expects that the system could not continue to supply drug to the surface to maintain the solubility limit. Thus, we applied a flux boundary condition as per Eq. 4 and carried out a similar derivation, obtaining a modified expression for dissolution rate (see Appendix).

$$-D\partial C/\partial z\Big|_{z=0} = k_s (C_0 - C) \tag{4}$$

Our approximate solution was verified by finite element simulations using FlexPDE v4.05a (PDE Solutions, Antioch, CA, USA). As demonstrated in the Appendix, the modified boundary condition allows the system to moderate the release of drug from the surface to a finite rate even in the hypothetical limit of infinite flow rate.

RESULTS AND DISCUSSION

Figure 2 superimposes the experimental results of the original study (7) on the same plot with the exact predictions of the former and current derivations. Although the data is not new, the comparison made in Fig. 2 is, as this plot enables a comparison between theory and experiment in absolute terms. This absolute comparison was lacking in the original study, which merely noted that the data exhibited the correct cube-root dependence on volumetric flow rate and the 2-fold change in dissolution rate upon rotating the orientation of the dissolving surface with respect to the direction of flow. In fact, when the comparison between the experiment release rate and the theoretical prediction assuming the solubility limit condition (infinite k_s) are made on an absolute basis using the values for solubility and diffusion coefficient given in Ref. 7 (6.262 millimolar and 9.86×10^{-10} $M^2 s^{-1}$, respectively), the data fall below the prediction by only 10%. Thus, it would

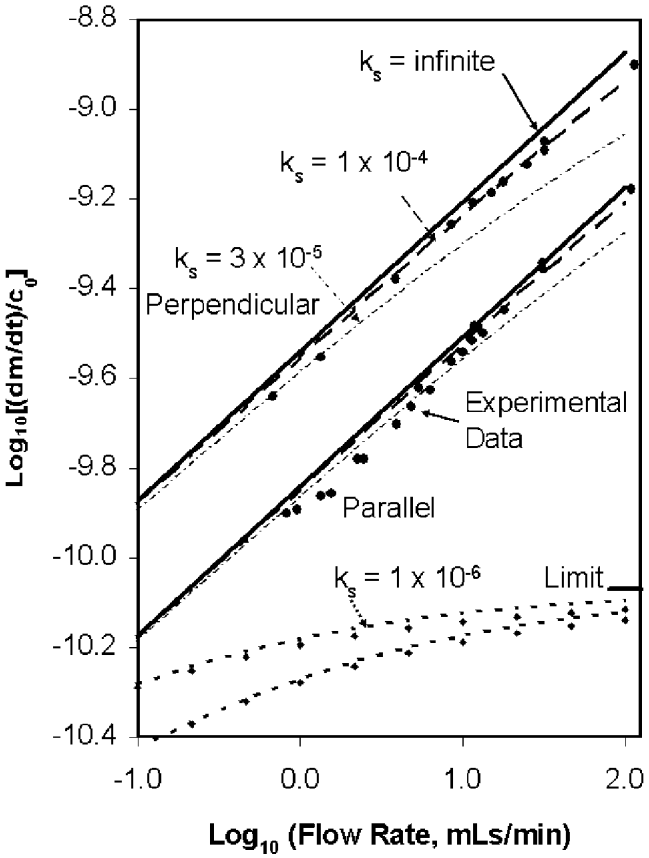

Fig. 2. Influence of flow rate and dye orientation on the dissolution of ethyl-*p*-aminobenzoate, data of Ref. 7, die attached to channel floor. Solid lines correspond to exact results calculated from Eq. 2, assuming the exposed drug surface concentration can be maintained at the solubility limit irrespective of flow rate. Remaining curves correspond to applying a limited flux condition, Eq. 4, on the exposed drug surface, where k_s represents an intrinsic dissolution rate constant, values indicated (units M s^{-1}). $k_s = 10^{-4}$; $k_s = 3 \times 10^{-5}$; $k_s = 10^{-6}$. In each case, the upper curve is for the die with the long axis of the opening oriented perpendicular to the direction of flow; the lower curve for the parallel orientation. Finite element simulation results are depicted as small points for the case $k_s = 10^{-6}$ only; for all other cases, simulation results superimpose upon the curves plotted. The limiting release rate at infinite flow rate from Eq. A15 for the case $k_s = 10^{-6}$ is also shown.

appear that for this compound and under the conditions of this dissolution experiment, the system has little difficulty maintaining the surface concentration very close to the solubility limit.

The investigators were apparently unaware of the very good absolute agreement between their experimental measurements and their theoretical predictions. This very slight disagreement might well be due to experimental uncertainty, or to geometric effects due to the finite channel width, diffusional broadening of dissolved solute, and so forth. Alternatively, it might instead be due to the limited rate at which material can dissolve from the surface, represented by a finite value for k_s. Superimposed upon the same plot are pairs of curves illustrating the impact of reducing the value of k_s below the infinite solubility limited value. As k_s diminishes, the dissolution rate also diminishes, with a more dramatic decrease as the flow rate increases. At first the impact of diminishing k_s provides only a small departure below the uppermost curve, and a slight decrease in the slope of the flow rate dependence, but eventually there is step curvature in the flow rate dependence. The curvature is more apparent for the case of the perpendicular orientation, with the net result that at the highest flow rates, the influence of changing orientation of the dissolving surface from perpendicular to parallel to the eluent flow also diminishes.

At extremely high flow rates, there eventually comes a point where the release rate becomes independent of further increases in shear rate or orientation of the releasing surface. For the case $k_s = 10^{-6}$, the limiting release rate is indicated in the figure. The estimate for the flow rate at which this occurs for the releasing surface oriented parallel to the flow direction is about 150 mLs/min, just to the right of the maximum abscissa value shown in the plot. This flow rate at which 90% of the theoretical maximum release rate is achieved (designated Q_{90} in the Appendix) varies as k_s^3 (Eq. A16). Thus, for $k_s = 10^{-4}$ (possibly a good fit to the trend in the experimental data), the Q_{90} flow rate is estimated to be one million times higher than this, an experimentally unapproachable limit.

The parameter k_s represents an intrinsic dissolution rate constant, similar to the constant k used in the USP intrinsic dissolution method (2), as per Eq. 5 (though not explicitly stated, is implied in the method), where dM/dt is the total rate of mass loss (same as R_{total})

$$dM/dt = -kA(C_0 - C) \tag{5}$$

from the exposed surface of area A. However, the parameter k_s more fundamentally reflects the intrinsic nature of the dissolution process. Unlike the USP intrinsic dissolution paradigm, which attributes the impact of hydrodynamics to be uniformly applied everywhere on the exposed drug surface, k_s is independent of hydrodynamics; it is area-independent and reflects only physicochemical factors.

It may be possible to separate intrinsic and extrinsic properties of the material and test apparatus as they impact the convective dissolution process, affecting solubility C_0, the flux parameter k_s, convective flow and solute diffusivity separately as follows:

Factors affecting solubility C_0: hydration, polymorphism, temperature, pH, eluent additives impacting solute solubility.

Factors affecting flux condition k_s: polymorphism, buffer capacity.

Factors affecting fluid convection: eluent bulk fluid viscosity, test apparatus geometry, disk (Wood's) or basket rotation speed/fluid flow rate (flow-through systems).

Factors affecting solute diffusivity: eluent additives (typically high concentrations of small hydrophilic molecules).

Note that in the laminar forced flow test system that the fluid velocity profile is independent of the bulk viscosity, which does not enter into the expression for shear rate in Eq. 3. The shear rate is a function only of the volumetric flow rate Q. The only impact of increasing bulk viscosity is to require more pressure to pump the fluid at a particular flow rate. However, bulk viscosity will impact the velocity profile and local shear rate in the vicinity of dissolving surfaces in stirred systems. We also distinguish between the effects of two separate types of eluent additives that impact the viscosity. Very

low concentrations of hydrophilic polymers can very efficiently increase bulk solution viscosity with negligible impact on dissolved solute diffusivity. Small molecules must be added in high concentration to significantly change eluent viscosity, and impact solute diffusivity by altering the microenvironment of the medium in which they diffuse. Additives can also impact the solubility of dissolved solute. These separate effects were very ably demonstrated in the later studies in the laminar channel by the same investigators (10,11).

CONCLUSIONS

Reexamination of the original experimental release rate data for ethyl-*p*-aminobenzoate in the laminar flow cell shows surprisingly good agreement when compared against theoretical prediction assuming the dissolving surface can be maintained at the solubility limit. The data fall slightly below this prediction, consistent with the possibility that a practical limit may be experienced. More data on a variety of compounds having disparate solubility and other properties would be required to establish the utility of the flux condition-derived intrinsic dissolution parameter k_s. One possible utility would be to provide a more realistic estimate of the duration of release under conditions of extreme flow, such as might be used in an attempt to accelerate the dissolution of a device near exhaustion in a finite and reasonable time.

The new intrinsic dissolution parameter is not limited to the simple rotating disc geometry, nor does it require impacting the drug source into a flat surface embedded in the wall of a flow cell. Rather, it may be deduced from any set of geometric and flow conditions, provided the fluid velocity distribution can be determined everywhere in the problem domain. This would be especially useful in situations where the analyst must test a finished dosage form of highly complex geometry. In fact, it should be possible to calculate numerically the dissolution rate for any object placed in any eluent flow field using the principles of convective diffusion/dissolution theory. This will be demonstrated and experimentally verified in the next article in this series (submitted to Pharmaceutical Development and Technology) for a different drug solute having very limited solubility, Anecortave Acetate.

ACKNOWLEDGMENT

The authors are indebted to Dr. Jamieson C. Keister of 3M, Pharmaceutics Department, St. Paul, Minnesota, for a critical review of the mathematical derivation in the Appendix.

APPENDIX

Derivation of an Approximate Solution. We found the example of solid dissolution into a falling film (12) was useful for correcting a misprint in the original derivation (8). In each case, the fluid velocity is constrained to one dimension, and velocity is assumed to vary linearly with distance away from the wall:

$$D\frac{\partial^2 C}{\partial z^2} = V_x\frac{\partial C}{\partial x} = \alpha\, z\frac{\partial C}{\partial x} \tag{A-1}$$

A solution of the following form for C is postulated:

$$C = \phi(\eta), \quad \eta \equiv z\left(\frac{\alpha}{9Dx}\right)^{\frac{1}{3}} \tag{A-2}$$

After applying the chain rule for differentiation, Eq. A1 becomes:

$$\frac{\partial^2\phi}{\partial\eta^2} + 3\eta^2\frac{\alpha\phi}{\partial\eta} = 0 \tag{A-3}$$

Integrating twice we obtain the following expression for $\phi(\eta)$:

$$\phi(\eta) = \gamma_1\int_0^{\eta} e^{-\beta^3}\, d\beta + \gamma_2 \tag{A-4}$$

The $\gamma_{1,2}$ are determined by the boundary conditions on x, which must be transformed into boundary conditions on η:

$$BC_1 : -D\frac{\partial C}{\partial z} = k_s\,(C_0 - C), \text{ at } 0 < x < L,\ z = 0$$

$$\rightarrow -D\frac{\partial\phi}{\partial\eta}\frac{\partial\eta}{\partial z} = k_s\,(C_0 - \phi) \text{ at } \eta = 0$$

$$BC_2 : C = 0 \quad \text{at} \quad x, z = \infty \quad \rightarrow \quad \phi = 0 \quad \text{at} \quad \eta = \infty$$

$$BC_3 : C = 0 \quad \text{at} \quad x = 0, z \quad \rightarrow \quad \phi = 0 \quad \text{at} \quad \eta = \infty$$

where BC_1 applies to the dissolving surface, and BC_2 fixes the concentration to be zero far away from the dissolving surface. BC_3 states that eluent entering from the inlet is devoid of drug and is identical to condition BC_2. Using Eq. A4 for $\phi(\eta)$ and making evaluations at $\eta = 0$, BC_1 becomes:

$$-D\left(\frac{\alpha}{9Dx}\right)^{\frac{1}{3}}\gamma_1 = k_s\,(C_0 - \gamma_2) \tag{A-5}$$

In the original problem (7,8) with a constant concentration for BC_1, the $\gamma_{1,2}$ were constants; however, in the current situation, in order to satisfy the boundary conditions, they must be functions of x. Thus, the function C(x,z) that we will obtain by this procedure will not satisfy the master differential equation Eq. A1, but will rather be an approximation. BC_2 provides a relation between γ_1 and γ_2:

$$\gamma_1\int_0^{\infty} e^{-\beta^3}\, d\beta + \gamma_2 = 0 \quad \rightarrow \quad \gamma_2 = -\gamma_1\,\Gamma\left(\frac{4}{5}\right) \tag{A–6}$$

Substituting this expression for γ_2 in Eq. A5, we obtain an expression for γ_1:

$$\gamma_1 = \frac{-C_0}{\Gamma\left(\frac{4}{3}\right) + \frac{D}{k_s}\left(\frac{\alpha}{9Dx}\right)^{\frac{1}{3}}} \tag{A–7}$$

Thus, the expression for concentration C(x,z) becomes:

$$C(x,z) \cong \frac{c_0}{\Gamma\left(\frac{4}{3}\right) + \frac{D}{k_s}\left(\frac{\alpha}{9Dx}\right)^{\frac{1}{3}}}\int_{\eta}^{\infty} e^{-\beta^3}\, d\beta \tag{A–8}$$

where $\eta(x,z)$ is given by Eq. A2, and where we have used the relations $\int_0^{\infty} = \int_0^{\eta} + \int_{\eta}^{\infty}$ and

$$\int_0^{\infty} e^{-\beta^3}\, d\beta = \frac{1}{3}\Gamma\left(\frac{1}{3}\right) = \Gamma\left(\frac{4}{3}\right) = 0.893 \tag{A–9}$$

When Eq. A8 is substituted in Eq. A1, all terms but one

cancel; the remaining term is premultiplied by the ratio (D/k_s) compared to the other terms which cancel. Because this ratio ranges between 10^{-5} and 10^{-3} for the values of D and k_s considered, there is hope that the approximation should be rather good. The accuracy of the approximation will shortly be demonstrated using finite element simulations.

The rate of dissolution R from the surface is:

$$\begin{aligned} R &= -D\left.\frac{\partial C}{\partial z}\right|_{z=0} \\ &= \frac{-Dc_0}{\Gamma\left(\frac{4}{3}\right)+\frac{D}{k_s}\left(\frac{\alpha}{9Dx}\right)^{\frac{1}{3}}}\left[\frac{\partial}{\partial z}\int_{\eta}^{\infty} e^{-\beta^3}\,d\beta\right]_{z=0} \\ &= \frac{+Dc_0}{\Gamma\left(\frac{4}{3}\right)+\frac{D}{k_s}\left(\frac{\alpha}{9Dx}\right)^{\frac{1}{3}}}\left[e^{-\eta^3}\frac{\partial\eta}{\partial z}\right]_{z=0} \\ &= \frac{+Dc_0}{\Gamma\left(\frac{4}{3}\right)+\frac{D}{k_s}\left(\frac{\alpha}{9Dx}\right)^{\frac{1}{3}}}\left(\frac{\alpha}{9Dx}\right)^{\frac{1}{3}} \\ &= \left(\frac{c_0 E}{1+\frac{1}{k_s}\left(\frac{1}{x}\right)^{\frac{1}{3}}E}\right)\frac{1}{x^{\frac{1}{3}}} \end{aligned} \tag{A-10}$$

where

$$E \equiv \frac{D^{\frac{2}{3}}\alpha^{\frac{1}{3}}}{9^{\frac{1}{3}}\Gamma\left(\frac{4}{3}\right)} \tag{A-11}$$

Expression Eq. A10 is very nearly proportional to $x^{-1/3}$. We can simplify this expression by substituting a constant ξ for one of the instances of x as follows:

$$R \cong \left(\frac{c_0 E}{1=\frac{1}{k_s}\left(\frac{1}{\xi}\right)^{\frac{1}{3}}E}\right)\frac{1}{x^{\frac{1}{3}}} \tag{A-12}$$

The sum of the mass loss rate over the entire surface is obtained by multiplying the local rate R by the width b and integrating over x from 0 to L. We choose ξ such that the contribution of dissolution upstream from ξ (on the interval from $0 < x < \xi$) is equal to the contribution downstream (the area underneath the function curve for $x^{-1/3}$ on the interval from zero to ξ is equal to the area on the interval from ξ to L):

$$\int_0^{\xi} x^{-\frac{1}{3}}\,dx = \int_{\xi}^{L} x^{-\frac{1}{3}}\,dx \tag{A-13}$$

The value of ξ which accomplishes this is $L/2/\sqrt{2}$. Thus, the total integrated mass dissolution rate over the dissolving surface is approximated by:

$$\frac{R_{total}}{c_0} \cong \left(\frac{3EbL^{\frac{2}{3}}}{2}\right) \Big/ \left(1+\frac{\sqrt{2}E}{k_s L^{\frac{1}{3}}}\right) \tag{A-14}$$

which reduces to the expression given by Eq. 2 of the text in the limit $k_s \to \infty$. Another useful result is the limit of expression Eq. A14 at infinite flow rate, which corresponds to infinite E:

$$\lim_{Q\to\infty} R_{total} = \lim_{E\to\infty} R_{total} = \frac{3}{2\sqrt{2}}bLk_s c_0 \tag{A-15}$$

This surprisingly simple result is independent of both shear rate and orientation of the releasing surface. (The result for the value boundary condition has no such limit, but assumes that the material can keep the surface concentration at the solubility limit irrespective of flow rate, leading to the unphysical consequence of infinitely rapid dissolution in the limit of infinite eluent flow rate.)

To obtain an estimate of the flow rate required to bring the system close to the intrinsic dissolution limit, we calculate the quantity E_{90} which will bring R_{total} to 90% of the limit of Eq. A15, and use expressions Eq. A12 and Eq. 3 of the text to obtain the corresponding flow rate Q_{90}, which evaluates to:

$$Q_{90} = \frac{3H^2WL}{4\sqrt{2}\,D^2}\left(9\Gamma\left(\frac{4}{3}\right)k_s\right)^3 \tag{A-16}$$

Confirmation by Finite Element Analysis. The domain selected for analysis was the section of the rectangular flow channel above the dissolving surface. The governing equation Eq. A1 was solved in the domain subject to boundary conditions as follows. The condition set along the x-axis at $z = 0$ (BC_1) was either value(concentration C) = 1 or outward flux = $k_s(1-C)$ (here we work in units of the drug solubility limit, assuming $c_0 = 1$). The condition set along the entire upper boundary at the top of the channel (BC_2) was value(C) = 0. The same zero concentration boundary condition was set on the left wall, representing the inlet of drugless eluent into the dissolving chamber (BC_3, now explicitly included). No condition was set on the right hand boundary.

Figure A1 shows a representative drug concentration profile for the steady-state solution in the case $k_s = 10^{-4}$ at a flow rate of 0.1 mLs/min. This solution is obtained by the software in just seconds of CPU time. The integral of the flux along the lower boundary for the constant concentration condition, when multiplied by the width of the releasing surface, provides a value which is within 0.2% of the exact expression given by Eq. 2 of the text over the entire range of flow rate from 0.1 to 100 mLs/min. This confirms that the numerical method is robust, and it is reasonable to trust its results when the flux condition is applied instead.

Figure A2 illustrates the comparison between the finite element solution and the approximate expression for C(x,z) given by Eq. A8 for the dissolving surface oriented with its long axis parallel to the direction of flow at a flow rate of 0.1 mLs/min. The comparison is made by plotting concentration as a function of x at two different values of z, for three different values of k_s. When $k_s = 10^{-4}$ or 10^{-5}, the agreement between the two solutions is within <1%; thus only a single curve is shown. For $k_s = 10^{-6}$, the approximation given by Eq. A8 deviates only a few percent above the finite element solution. Thus it is demonstrated that despite the fact that Eq. A8 does not strictly satisfy the differential equation Eq. A1, it nevertheless provides a reasonable approximation to the real solution, at least for $D/k_s \leq 10^{-3}$.

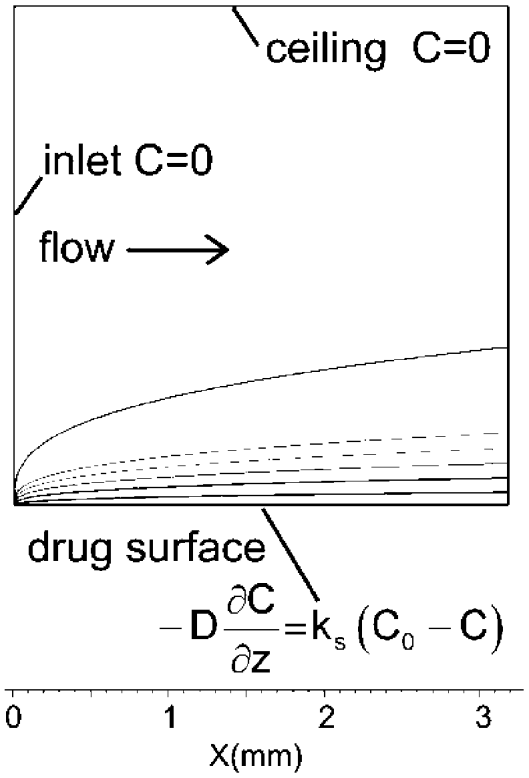

Fig. A1. Finite element simulation of drug concentration in the channel above the releasing surface for the case of the rectangular surface oriented with the long axis perpendicular to the direction of flow, case $k_s = 10^{-4}$ at a flow rate of 0.1 mLs/min. Each contour represents an increase of 10% of the drug solubility limit c_0; thus, the uppermost contour corresponds to $C = 0.1 * c_0$; the lowest contour just above the $z = 0$ axis corresponds to $C = 0.9 * c_0$; and so forth. Dimensions are in millimeters. Boundary conditions are shown.

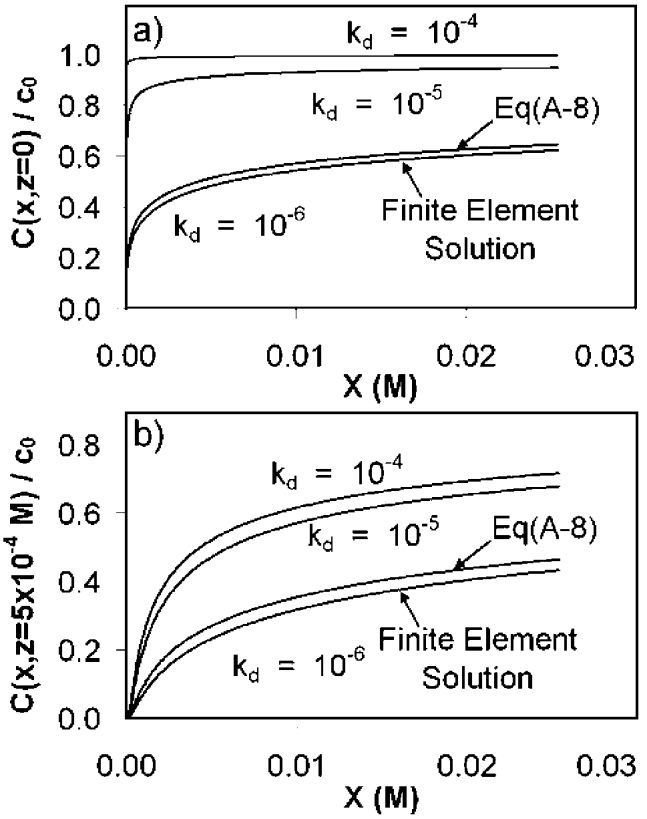

Fig. A2. X-dependence of the steady-state drug concentration at two fixed values of z for orientation with the long axis parallel to the direction of flow, comparing the approximate solution given by Eq. A8 with the finite element solution (indistinguishable for $k_d = 10^{-4}$, 10^{-5}). (a) Concentration at $z = 0$ (along the dissolving surface). (b) Concentration at a height of $z = 0.5$ mm above the surface.

For the flux condition cases $k_s = 10^{-4}$ and $k_s = 3 \times 10^{-5}$, the total flux reported by the finite element method is with 0.5% or less of the approximate expression given by Eq. A14 over the entire range of flow rate for either orientation, and if plotted would superimpose perfectly upon the curves in Fig. 2. The worst disagreement occurs at the highest flow rates for the case $k_s = 10^{-4}$, in which the simulated flux falls below the approximation by 5% or less. Thus, we assert that the approximation for the flux given by Eq. A14 is accurate to within 5% over the entire range of flow rate from 0.1 to 100 mLs/min and flux parameter $1 \times 10^{-6} < k_s < \infty$.

Expression of the Approximation as a Valid Solution to the PDE. We can overcome one objection that might be raised to the closed form approximation of Eq. A8, that it does not strictly satisfy the partial differential equation given by Eq. A1, by introducing the variable ξ earlier in the derivation. By substituting $L/2\sqrt{2}$ for x in Eq. A5, we obtain:

$$-\sqrt{2}\,D\left(\frac{\alpha}{9DL}\right)^{\frac{1}{3}}\gamma_1 = k_s\,(C_0 - \gamma_2) \qquad \text{(A-5′)}$$

This removes the x-dependence from the parameters $\gamma_{1,2}$, allowing Eq. A8 to be expressed as follows:

$$C(x,z) \cong \frac{c_0}{\Gamma\left(\frac{4}{3}\right) + \frac{\sqrt{2}\,D}{k_s}\left(\frac{\alpha}{9DL}\right)^{\frac{1}{3}}}\int_{\eta}^{\infty} e^{-\beta^3}\,d\beta \qquad \text{(A-8′)}$$

This equation is indeed a valid solution to Eq. A1, and produces the same expressions for the release rate given by Eqs. A12 and following. However, it does not appear to provide as accurate a description of the spatial dependence of concentration near the releasing surface as does the original expression Eq. A8 when compared with elevation plots of the finite element solution close to the surface.

Finite Element Simulation of Parabolic Velocity Flow Profile. Of potential concern is the fact that the linear velocity profile is only a reasonable assumption in the vicinity of the releasing surface, representing the limiting slope of the parabolic Poiseuille-type flow occurring in the channel. The linear velocity profile would require a non-zero velocity at the upper channel boundary, which is unphysical. A more physically reasonable velocity profile would be given by the following expression, assuming that the distance between the inlet and the releasing surface was long enough to establish the parabolic profile:

$$V_x = \frac{H\alpha}{4}\left[1 - \left(\frac{2z - H}{H}\right)^2\right] \qquad \text{(A-17)}$$

The linear velocity profile used in Eq. A1 is obtained by taking the derivative of this expression with respect to z and evaluating the result at $z = 0$. In principle it would be possible to obtain the solution to the differential equation Eq. A1 in which expression Eq. A17 would be substituted for V_x:

$$D\frac{\partial^2 C}{\partial z^2} - \frac{H\alpha}{4}\left[1 - \left(\frac{2z - H}{H}\right)^2\right]\frac{\partial C}{\partial x} = 0 \qquad \text{(A-18)}$$

Finite element simulations suggest that the effort of such a derivation would hardly be justified. The impact of the parabolic velocity profile reduces R_{total} by only a small amount, with the largest effect being observed at the slowest flow rates. The reduction at 0.1 mLs/min is only 10% for the parallel orientation and 4% for the perpendicular orientation. The effect is greatly diminished as the flow rate increases, since the upward extant of the drug concentration profile becomes greatly diminished with increasing flow rate.

REFERENCES

1. USP 26 section <711> Dissolution, pp. 2155–2156.
2. USP 26 section <1087> Intrinsic Dissolution, pp. 2333–2334.
3. USP 26 section <724> Drug Release, pp. 2157–2165.
4. The Anecortave Acetate Clinical Study Group. Anecortave acetate as monotherapy for treatment of subfoveal neovascularization in age-related macular degeneration (AMD): 12 month clinical outcomes. *Ophthalmol.* **110**:90–101 (2003).
5. J. H. Wood, J. E. Syarto, and H. Letterman. Improved holder for intrinsic dissolution rate studies. *J. Pharm. Sci.* **54**:1068 (1965).
6. N. Khoury, J. W. Mauger, and S. Howard. Dissolution rate studies from a stationary disk/rotating fluid system. *Pharm. Res.* **5**: 495–500 (1988).
7. A. C. Shah and K. G. Nelson. Evaluation of a convective diffusion drug dissolution rate model. *J. Pharm. Sci.* **64**:1518–1520 (1975).
8. K. G. Nelson and A. C. Shah. Convective diffusion model for a transport-controlled dissolution rate process. *J. Pharm. Sci.* **64**: 610–614 (1975).
9. V. Levich. *Physicochemical Hydrodynamics*, Prentice-Hall, Englewood Cliffs, NJ, 1962, p. 48.
10. K. G. Nelson and A. C. Shah. Mass transport in dissolution kinetics I: Convective diffusion to assess the role of fluid viscosity under force flow conditions. *J. Pharm. Sci.* **76**:799–802 (1987).
11. A. C. Shah and K. G. Nelson. Mass transport in dissolution kinetics II: Convective diffusion to assess role of viscosity under conditions of gravitational flow. *J. Pharm. Sci.* **76**:910–913 (1987).
12. P. J. Missel, L. E. Stevens and J. W. Mauger. Dissolution of anecortave acetate in a cylindrical flow cell: re-evaluation of convective diffusion/drug dissolution for sparingly soluable drugs. *Pharm. Dev. Tech.* **9**:453–459 (2004).
13. R. B. Bird, W. E. Stewart, and E. N. Lightfoot. *Transport Phenomena*, Wiley, New York, 1960, pp. 551–552.